

Proteomic characterization of histone variants in the mouse testis by mass spectrometry-based top-down analysis

Ho-Geun Kwak^{1,2}, Naoshi Dohmae^{1,2,*}

¹Biomolecular Characterization Unit, RIKEN Center for Sustainable Resource Science, Hirosawa, Wako, Japan;

²Graduate School of Science and Engineering, Saitama University, Saitama, Japan.

Summary Various histones, including testis-specific histones, exist during spermatogenesis and some of them have been reported to play a key role in chromatin remodeling. Mass spectrometry (MS)-based characterization has become the important step to understand histone structures. Although individual histones or partial histone variant groups have been characterized, the comprehensive analysis of histone variants has not yet been conducted in the mouse testis. Here, we present the comprehensive separation and characterization of histone variants from mouse testes by a top-down approach using MS. Histone variants were successfully separated on a reversed phase column using high performance liquid chromatography (HPLC) with an ion-pairing reagent. Increasing concentrations of testis-specific histones were observed in the mouse testis and some somatic histones increased in the epididymis. Specifically, the increase of mass abundance in H3.2 in the epididymis was inversely proportional to the decrease in H3t in the testis, which was approximately 80%. The top-down characterization of intact histone variants in the mouse testis was performed using LC-MS/MS. The masses of separated histone variants and their expected post-translation modifications were calculated by performing deconvolution with information taken from the database. TH2A, TH2B and H3t were characterized by MS/MS fragmentation. Our approach provides comprehensive knowledge for identification of histone variants in the mouse testis that will contribute to the structural and functional research of histone variants during spermatogenesis.

Keywords: Testis-specific histones, top-down analysis, mass spectrometry

1. Introduction

Several histones have been detected in mammalian testes and testis-specific variants are specifically and highly expressed during spermatogenesis (1-3). Testis-specific histones (H1t, TH2A, TH2B, and H3t) are related to dynamic chromatin remodeling during the histone-to-transitional protein stage as well as their functional roles, such as fertility (1-3). For example, our recent study indicated that the lack of Th2a and Th2b encoding TH2A and TH2B, respectively, resulted in sterility in male mice, and the loss of TH2A and TH2B was linked

with cohesion release and histone replacement during spermatogenesis (4). Additionally, linker testis-specific histone H1t revealed that there was no influence on male mice fertility (5). There is some evidence that testis-specific histone H1t and H3t are linked with chromatin remodeling during spermatogenesis, but further research to investigate the relationship with testis-specific histone variants such as H3t is still needed (3).

Studies for characterization of testis-specific histones are essential to trace epigenetic activities of histone variants. Some studies on the characterization of individual testis-specific histones during spermatogenesis have been reported. Lu *et al.* discovered the mass value for TH2B from mice as well as those for different TH2B post-translational modifications (PTMs) present during spermatogenesis using Liquid chromatography (LC)-mass spectrometry (MS) with trypsin digestion (6). Additionally, studies have reported that LC-MS enabled characterization of TH2B expression patterns during mouse spermatogenesis (4,7). However, research

Released online in J-STAGE as advance publication August 19, 2016.

*Address correspondence to:

Dr. Naoshi Dohmae, Biomolecular Characterization Unit, RIKEN Center for Sustainable Resource Science, 2-1 Hirosawa, Wako, 351-0198, Japan.
E-mail: dohmae@riken.jp

involving MS-based characterization of histone variants in mouse testes is limited in comparison to functional studies. The elucidation of comprehensive analytical approaches for functional research into testis-specific histone variants is imperative.

MS-based proteomic analysis has become a universal and powerful tool enabling the characterization of peptides and proteins. This method has conventionally relied upon a bottom-up strategy due to its excellent sensitivity. However, the digestion processes associated with active enzymes hinder extensive characterization of intact proteins, resulting in the loss of significant information pertaining to the sequencing of histone proteins due to the availability of only extremely short peptide sequences. For this reason, a top-down technique that enables characterization of intact proteins is used (8-11). LC in top-down strategies is generally utilized for the separation of intact proteins using reversed phase (RP) columns (C4, C8, and C18). In particular, columns designed for shorter alkyl groups are traditionally used in top-down approaches due to the intensive nature of the recovery techniques (8,10). Improvements in methods addressing the technical and structural challenges for relationships to intact-protein separation are feasible and necessary for the development of analytical sensitivity in columns (10,12). Likewise, ion-pairing reagents, such as trifluoroacetic acid (TFA), pentafluoropropionic acid, and heptafluorobutyric acid (HFBA), are useful in reducing the hydrophilicity of proteins and peptides through interactions with anions, resulting in enhanced resolution of RP columns. Shibue *et al.* reported that the efficiency of peptide separation was enhanced by strengthening the hydrophobicity of the reagent. Specifically, HFBA showed the most sensitive and intensive signals in results from RP chromatography when compared with other ion-pairing reagents (13).

Here, we report the comprehensive characterization of histone variants in mouse testes by MS-based proteomic analysis. The separation of histone variants in the mouse testis was performed by HPLC on the RP-column with HFBA as ion-pairing reagent. The top-down characterization of intact histone variants in the mouse testis was performed by LC-MS. Masses of separated histone variants and their expected PTMs were calculated by deconvolution based on the database. TH2A, TH2B and H3t were characterized by MS/MS fragmentation.

2. Materials and Methods

2.1. Materials

Trichloroacetic acid (TCA), hydrochloric acid (HCl), potassium chloride (KCl) magnesium acetate ($\text{Mg}(\text{CH}_3\text{COO})_2$) and dithiothreitol (DTT) were purchased from Wako Pure Chemicals (Osaka, Japan). Trizma base was from Sigma-Aldrich (St Luis, MO,

USA) and sulfuric acid (H_2SO_4) was obtained from Junsei Chemical Co. (Tokyo, Japan). HFBA (Thermo-Fisher Scientific, Waltham, MA, USA), TFA (Merck, Darmstadt, Germany) and acetonitrile (Thermo-Fisher Scientific, Waltham, MA, USA) were of HPLC reagent grade.

2.2. Extraction of histones from mouse testes

Mouse (BALB/c) testes combined with epididymides were purchased from Funakoshi Co. (Tokyo, Japan), and were homogenized following separation. Whole histones in testis and epididymis were extracted using the TCA-precipitation method with minor modifications (14). In brief, all steps were carried out at 4°C. Testis (49.1 mg) and epididymis (50.4 mg) were suspended in hypertonic lysis buffer [10 mM Tris-Cl (pH 8.0), containing 1 mM KCl, 1.5 mM $\text{Mg}(\text{CH}_3\text{COO})_2$, 1 mM DTT, and protease inhibitors] and then incubated for 30 min. Lysed cells were pelleted by centrifugation at $10,000\times g$ for 10 min, re-suspended in 0.4 N H_2SO_4 , and incubated for 30 min. To collect the supernatant containing histones, the nuclear debris in these samples was purified by centrifugation at $16,000\times g$ for 10 min and the supernatant was precipitated by TCA and incubated for 30 min. The precipitated samples were pelleted by centrifugation at $16,000\times g$ for 10 min. After washing with acetone and drying at room temperature, samples were mixed with 100 μL MilliQ water.

2.3. Separation of histone variants

Histones, including testis histones, were separated by an Agilent 1100 series HPLC (Agilent Technologies, Snata Clara, CA, USA) using a WP300 C4 column (2.0 mm \times 15.0 mm, 3- μm particle size; GL sciences, Tokyo, Japan) at room temperature. A 20- μL sample was injected and detected at a UV wavelength of 215 nm. HFBA was used as an ion-pairing reagent. The mobile phase A (5% acetonitrile with 0.1% HFBA) and B (90% acetonitrile with 0.1% HFBA) were delivered at a flow rate of 0.1 mL/min using the following gradient parameters: 0 min (to 5 min, 15% solvent B); 5 min (to 15 min, 15-48% solvent B); 15 min (to 25 min, 48% solvent B); 25 min (to 100 min, 48-62% solvent B); 100 min (to 120 min, 62-100% solvent B); 120 min (to 130 min, 100% solvent B); 130 min (to 135 min, 100-15% solvent B); 135 min (to 145 min, 15% solvent B). The fraction collector (Gilson, Middleton, WI, USA) was programmed to collect fractions at 1-min intervals from 30 min to 116 min.

2.4. Top-down analysis

Separated histones were analyzed by a Q-Exactive mass spectrometer (Thermo-Fisher Scientific, Bremen, Germany) using a linear gradient of 0-100% solvent

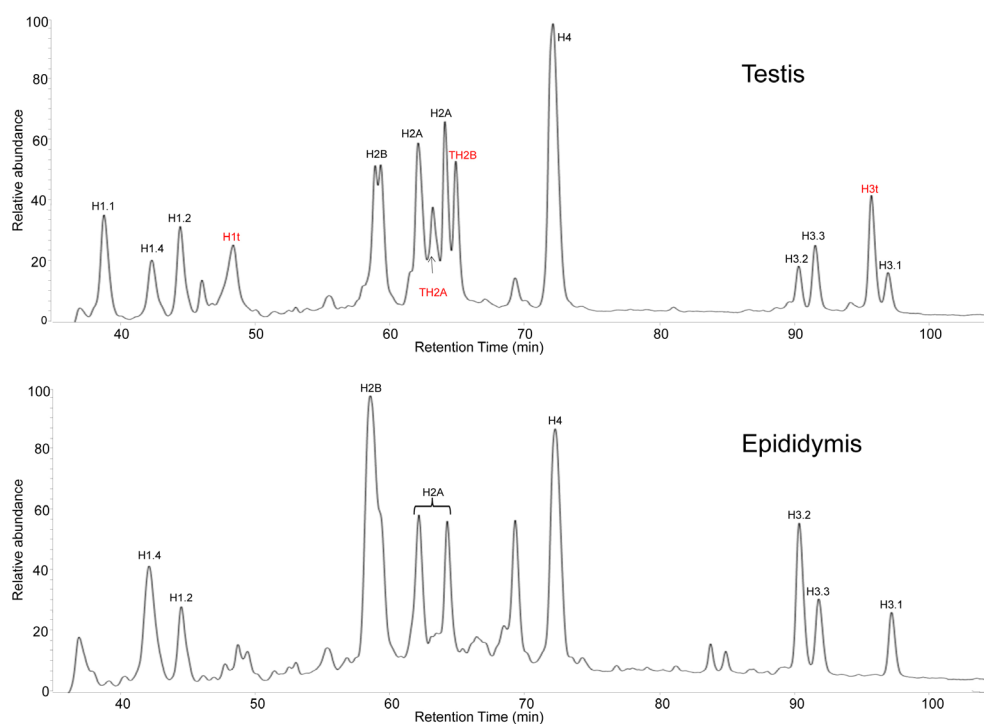


Figure 1. Chromatograms of histones in the mouse testis and epididymis. Histones from mouse testis (top) and epididymis (bottom) were separated using a C4 RP column with HFBA. Each signal was identified by PMF in advance (see Supporting Information).

B over 30 min (solvent A: 0.1% TFA; solvent B: 80% acetonitrile with 0.1% TFA). A flow rate of 300 nL/min was used with a 100 $\mu\text{m} \times 12$ cm silica capillary column in-house packed with InertSustainSwift C18 (3- μm particle size; GL sciences, Tokyo, Japan). MS was directed using Xcalibur software version 3.0.63 (Thermo-Fisher Scientific, Bremen, Germany). A nanoelectrospray (Thermo-Fisher Scientific, Bremen, Germany) was applied with a 1.9 kV spray voltage and a capillary temperature of 275°C. MS data were obtained in the range of 400-2,000 m/z with a resolution of 35,000 (at 400 m/z). Q-Exactive data were deconvoluted using software (Thermo-Fisher Scientific, Bremen, Germany). MS/MS analysis was performed by higher-energy collisional dissociation (HCD) fragmentation. Three or four precursor ions representing the most abundant charge states were targeted in HCD mode from MS spectra. Precursor ion mass spectra were collected in the range of 400-2,000 m/z with a resolution of 70,000 (at 400 m/z).

2.4. Data analysis

Each histone variant fraction was identified by peptide-mass fingerprinting (PMF) in advance (Supporting Information). The sequences of histone variants and their modifications were searched against a database (NCBIInr) and another study for H3t (15). Theoretical masses and MS/MS fragments were accomplished using the GPMW 6.1 software (Lighthouse data, Odense, Denmark) and MS/MS spectra of TH2A,

TH2B and H3t were manually characterized. The mass values of histone variants with their modifications from MS spectra were calculated by deconvolution software (Protein deconvolution version 3.0, Thermo-Fisher Scientific, Bremen, Germany) with the following conditions; a resolution of 35,000 in the range of 400-2,000 m/z (at 400 m/z) and S/N threshold of 3.

3. Results

3.1. Separation of histone variants by ion-pairing chromatography

Figure 1 shows chromatograms of separated histones from mouse testis and epididymis. Several histones were separated from the sample on the WP300 C4 column using HFBA as an ion-pairing reagent. Separated fractions were identified by PMF in advance and data was searched against a protein database search (NCBIInr) using the MASCOT search engine (Supporting Table 1, see Supporting Information, <http://www.biosciencetrends.com/docindex.php?year=2016&kanno=5>). Here, we successfully separated each histone from the mouse testis and epididymis using an RP column with HFBA. We observed testis-specific histones in mouse testis; however, their concentrations were undetectable in the epididymis (Figure 1). Some somatic histone variants were increased in the epididymis. Specifically, signals denoting H2B and H3.2 remarkably increased in the epididymis as compared with the deficient levels of TH2B and H3t from the testis (Figure 1). The loss of H3t

in the mouse testis was compensated by somatic histone H3 variants in the epididymis (Figure 1 and Table 1). Interestingly, H3.2 mainly showed the proportional offset as 79.1% in the epididymis, as compared to H3t deficiency from the mouse testis (Table 1). In our results, we isolated H1t along with other H1 variants (H1.1, H1.2, and H1.4) from mouse testis. Additionally, H1.1 and H1t deficiency and increased levels of H1.4 were observed (Figure 1).

3.2. MS-based identification of intact histone variants

Separated intact histone variants from the mouse testis

Table 1. Quantification of H3 variants based on areas of peaks

Histone	Areas (Average \pm S.D., %)	
	Testis	Epididymis
H3.2	16.5 \pm 1.0	52.9 \pm 0.2
H3.3	22.6 \pm 0.04	26.5 \pm 0.4
H3t	46.0 \pm 0.8	ND
H3.1	14.8 \pm 0.2	20.5 \pm 0.3

ND: Not detected; Areas of H3 variants were calculated from the integrated peaks on chromatograms and were expressed as percentages relative to the total peak area. The data is shown as averages with SD ($n = 3$). H3.2 was mainly compensated in the epididymis as approximately 80% in comparison with the loss of H3t in the testis.

and epididymis were identified by a Q-Exactive mass spectrometer, followed by deconvolution of the data. Table 2 displays the list of somatic and testis-specific histones from the mouse testis. The observed masses of the intact histones were compared with their theoretical masses, which matched their known sequences and expected PTMs. Our results indicated that the deconvoluted masses of four testis-specific histones (H1t, TH2B, TH2A and H3t) were in agreement with their theoretical masses (~ 0.11 Da). Additionally, the monoisotopic masses of somatic histones from the mouse testis, such as, H2B variants (H2B1F, H2B1B, and H2B1C), H2A variants (H2A1, H2A2A, H2A3, H2A.X, and H2A.Z), H3 variants (H3.1, H3.2, and H3.3), and H4, were calculated with accuracy (Table 2).

We used a Q-Exactive mass spectrometer for the characterization of testis-specific histones (TH2A, TH2B and H3t) with each histone fragmented in HCD mode. Figure 2 shows an example of the TH2B characterization process. Larger masses observed in the MS spectrum were targeted as fragmentation sources. A total of 20 y and b ions associated with TH2B were generated in HCD mode, and these fragmented ions were matched in the MS/MS spectrum with the TH2B sequence. Similarly, the mapping of other testis-specific histones was conducted from the HCD fragmentation of precursor ions in the range of 400 m/z

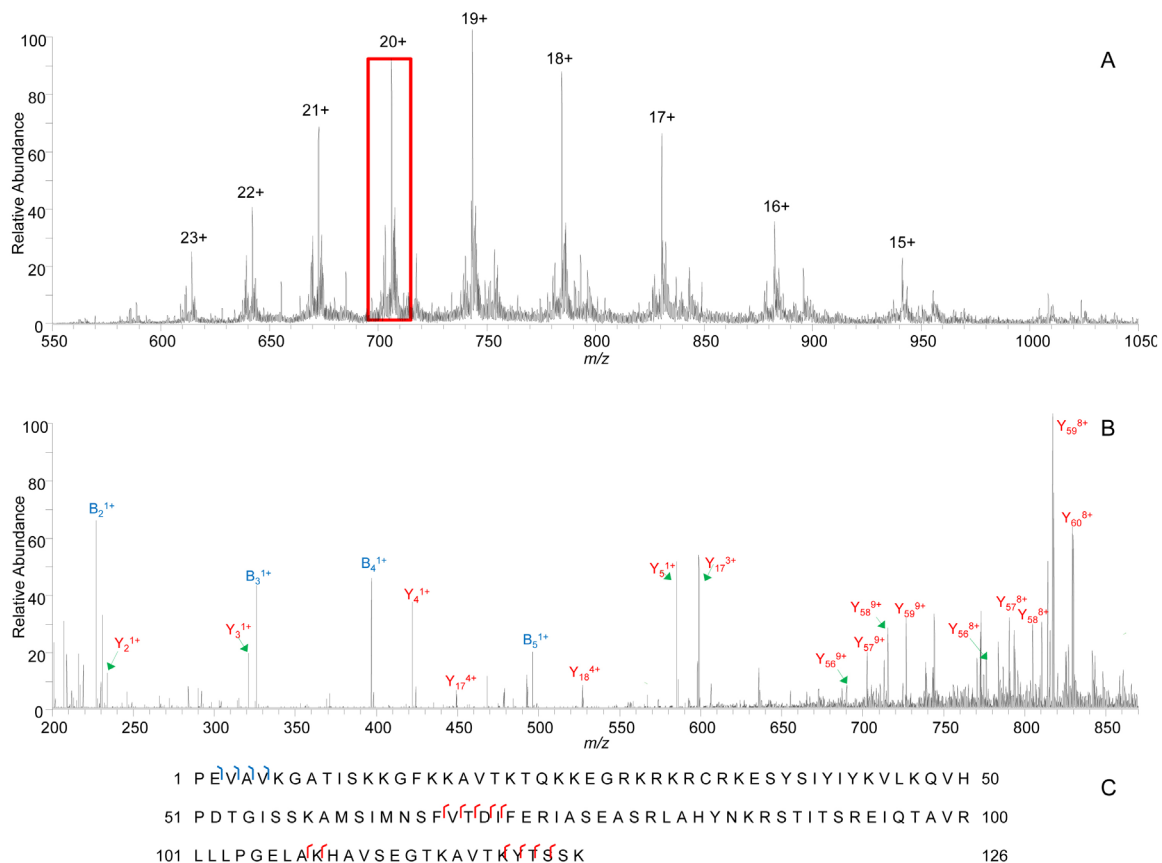


Figure 2. Top-down MS-based characterization of TH2B from mouse testis by HCD fragmentation. (A) MS spectrum of TH2B. Major precursor ions were targeted for MS/MS analysis. **(B)** HCD spectrum of precursor ions ($z = 20$) with matching b and y fragments. **(C)** Mapping HCD fragments of TH2B at the 20+ charge state.

Table 2. List of histone variant masses in the mouse testis

Histones	Accession	PTMs	Theoretical mass (Da)	Observed mass (Da)	ΔDa
H1t	Q07133	N-terminal acetylation	21438.12	21438.19	0.07
H2B1F	P10853	None	13796.53	13796.56	0.03
H2B1B	Q64475	None	13812.52	13812.55	0.03
H2B1C	Q6ZWY9	None	13766.52	13766.54	0.02
TH2B	P70696	None	14096.71	14096.79	0.08
H2A1	P22752	N-terminal acetylation	14037.92	14037.95	0.03
H2A2A	Q6GSS7	N-terminal acetylation	13997.86	13997.89	0.03
H2A3	Q8BFU2	N-terminal acetylation	14023.90	14023.92	0.02
H2A.Z	P0C0S6	None	13413.51	13413.48	0.03
H2A.X	P27661	N-terminal acetylation	15044.41	15044.44	0.03
TH2A	Q8CGP4	N-terminal acetylation	13958.83	13958.86	0.03
H4	P62806	N-terminal acetylation, Dimethylation	11299.38	11299.42	0.04
H3.1	P68433	5 methylation	15333.52	15333.63	0.11
H3.2	P84228	5 methylation	15317.54	15317.65	0.11
H3.3	P84244	4 methylation	15243.52	15243.64	0.12
H3t	.	4 methylation	15344.49	15344.60	0.11

Theoretical masses were calculated by the software based on reported sequence and their PTMs from the database and another study (H3t) (15). Observed masses are displayed as the most abundant form from the deconvoluted MS spectra.

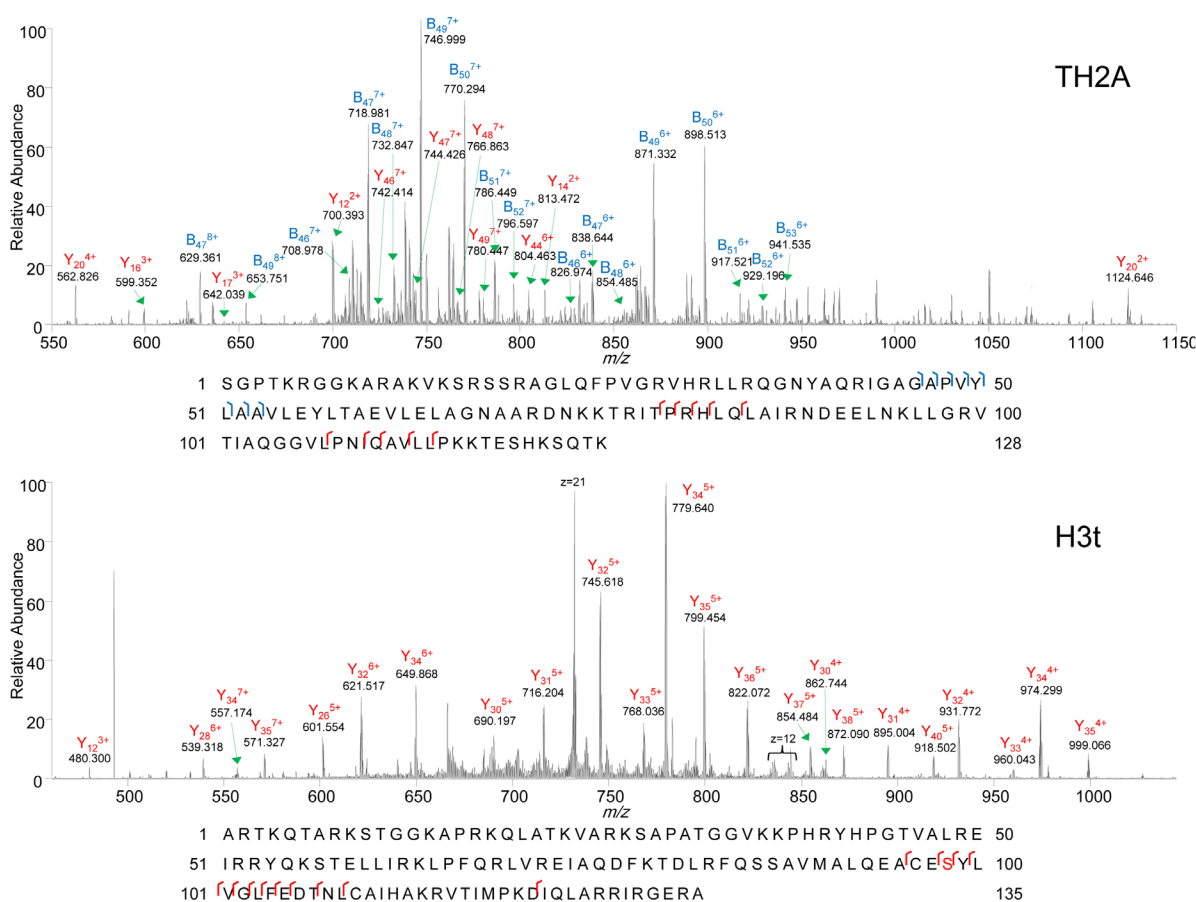


Figure 3. The mass spectra and sequences of TH2A and H3t. TH2A and H3t were characterized by HCD fragmentation. The sequences of histone variants were searched against the database (NCBIInr) and another study (15).

to 2,000 *m/z*. Peaks in the 736.11 *m/z* (*z* = 19) range for TH2A and 732.13 *m/z* (*z* = 21) for H3t were selected for fragmentation, with the *y*- and *b*-ion fragments corresponding to TH2A and H3t sequences (Figure 3). We also found fragments of H1t, which were in agreement with *y* ions associated with its C-terminal region (data not shown).

3.3. PTMs of testis-specific histone variants in mouse testis

Figure 4 shows PTMs of histones in the mouse testis. Histone PTMs were calculated by deconvolution according to the MS spectra and our results revealed specific PTMs (methylation, acetylation and

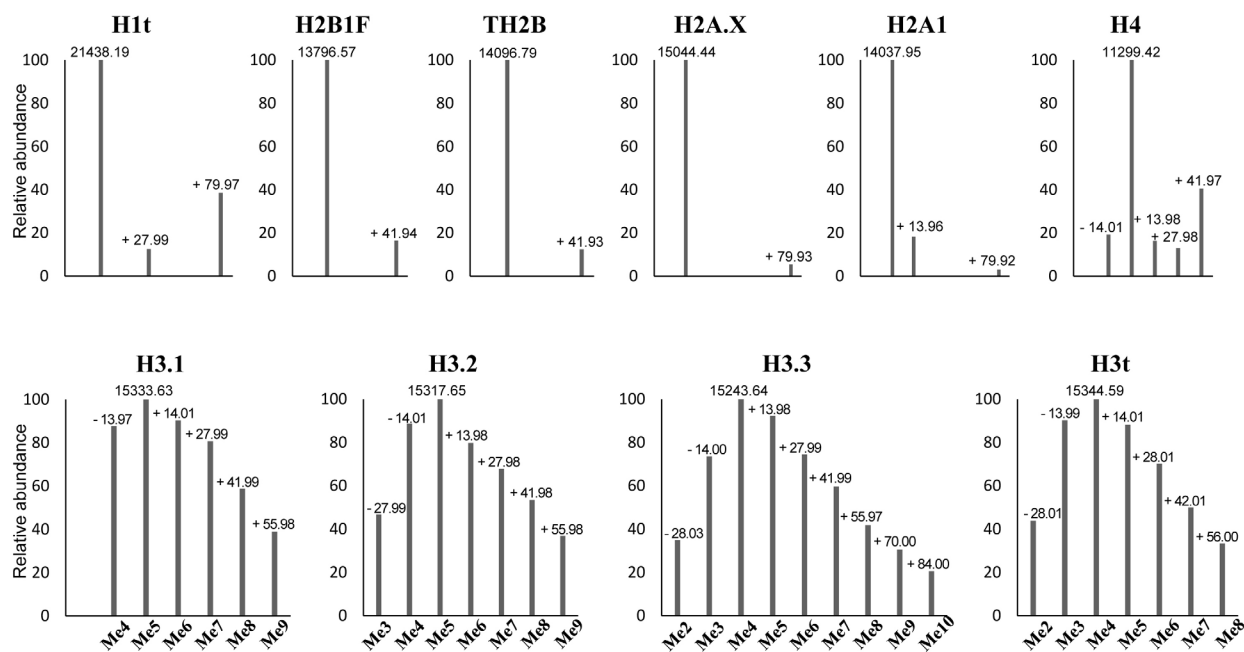


Figure 4. PTMs on histone variants from mouse testis. Me: methylation; The most abundant monoisotopic masses and mass differences were calculated using deconvolution. Acetylated N-termini of H1t, H2A1, H2A.X, and H4 (with dimethylation) were observed as the most abundant masses. 5 methylated H3.1 and H3.2 and 4 methylated H3.3 and H3t histones were detected as the most abundant monoisotopic masses. +13.96 Da (monomethylation), +27.99 Da (dimethylation), ~+41.93-+41.97 Da (trimethylation or acetylation), and ~+79.92-+79.97 Da (phosphorylation) were detected on H1t, H2B1F, TH2B, H2A.X, H2A1, and H4. The values of methylation of H4 and H3 variants were counted on the basis of their mass shifts from the most abundant masses. For example, the masses of -13.99 Da and +14.01 Da indicated trimethylation and 5 methylation in H3t, respectively.

phosphorylation) on somatic and testis-specific histones (Figure 4). Here, we calculated changes in masses of ~13.96-14.01 Da for methylation from H2A1 and H4, ~27.98-27.99 Da for dimethylation from H1t and H4, ~41.93-41.97 for trimethylation or acetylation from H2B1F, TH2B, and H4, and ~79.92-79.97 Da for phosphorylation from H1t, H2A.X and H2A1 in the mouse testis (Figure 4). In addition, higher abundances of methylation were observed in H3 variants (Figure 4). 5 methylated H3.1 and H3.2 and 4 methylated H3.3 and H3t histones were detected as the most abundant monoisotopic masses by deconvolution and other methylations were also observed in H3 variants (Figure 4). The values of methylations of H3 variants were counted on the basis of their mass shifts from the most abundant masses. For example, the masses of -13.99 Da and +14.01 Da indicated trimethylation and 5 methylation in H3t, respectively (Figure 4).

4. Discussion

Various histone variants as well as their PTMs are related to chromatin remodeling during spermatogenesis (1-3). To understand their structural patterns related to chromatin dynamics, an MS-based characterization process is required. Some studies have reported the MS-based characterization on individual histone variants (4,6,7). However, it is difficult to find the comprehensive identification of intact histones in the mouse testis. Here, we separated histone variants from the mouse testis and

conformed their replacement patterns in the epididymis. Each separated intact histone was identified using LC-MS/MS. Specifically, we conformed testis-specific histone's sequences by HCD fragmentation.

The separation of histone variants is an essential step for the structural research of histone proteins or their PTMs. We used HFBA as the ion-pairing reagent for histone separation in this study. Ion-pairing reagents play an important role in the RP-column separation of proteins and peptides in accordance with their hydrophobicity by causing interactions with protein side chains. Specifically, HFBA showed the best sensitivity and intensity in peptide-separation results when compared to other ion-pairing reagents (13,16). We successfully separated each testis-specific histone in this study. Moreover, our results showed a better separation efficiency, as compared to our previous research when we used TFA as the ion-pairing reagent (4).

Testis-specific histones, H1t, TH2A, TH2B and H3t, are abundant in mammalian testes and they gradually decrease during the histone-to-protamine stage by chromatin remodeling (1-3). The mouse epididymis is a tube connected to the testis where mature sperm is stored and transported (2). In this study, it was used to compare the histone dynamics between the testis and epididymis in mice. We observed the expression of testis-specific histones in the mouse testis and they were undetected in the mouse epididymis. To trace the transformed testis-specific histones as somatic types is also important to understand histone dynamics during spermatogenesis.

H1t is normally observed during spermatogenesis and somatic histone H1 variants are detected in H1t-deficient mice (2,5,17). An increased concentration of somatic histone H2B was observed in TH2B knock-out mice during spermatogenesis in our previous research (4). Our results showed compensated signals in the epididymis, as compared to the loss of testis-specific histones. Specifically, H3.2 was proportionally offset against the H3t deficiency in the epididymis. Histone H3t is highly expressed during spermatogenesis and observed at lower concentrations in somatic cells (2,3,18). However, the level of H3t was not observed in the mouse epididymis in this research. The relationship between H3t and other H3 variants in the testis has not been fully reported. Although further research concerning the compensatory nature of testis-specific histone expression is needed, our results indicating possible correlations between expression levels may provide unique and invaluable insight into the functional roles.

To characterize separated intact testis-specific histones, we used MS-based top-down analysis. Various histones including testis-specific histones and somatic histones coexist in the testis and some variants have similar sequences (1). For example, H3t shows only three different amino acids in its sequence in comparison with the canonical H3 (15). The MS-based top-down approach is suitable for comprehensive characterization of intact histones because the proteins' sequences and their PTMs are conserved (8-11,19). Previous research explored the use of proteomic analysis techniques and MS to identify the mass of TH2B (4,6,7); however, the results were not sufficiently comprehensive enough to verify MS-based characterization of testis-specific histones. In this study, we showed comprehensive analysis of histone variants in the mouse testis by the MS-based top-down approach. Additionally, we performed the characterization of testis-specific histones by sequencing using HCD fragmentation. HCD is similar to collision-induced dissociation (CID), and both fragmentation approaches are useful tools for identifying intact proteins with highly similar sequences. Moreover, HCD is more sensitive and allows for higher resolution of results relative to CID (8,10). Despite interest in functional and structural research of testis-specific histones, data associated with their MS-based characterization has been ambiguous. Our results presented successful sequence-based characterization of testis-specific histones from mice.

In this study, some PTMs on histone variants in the mouse testis were detected by MS-based top-down characterization. PTMs in male germ cells play a key role in biological activities related to chromatin remodeling, and can be found on histone proteins in the form of methylation, acetylation, phosphorylation, or ubiquitination (2,3,20). In particular, various mass shifts were observed from the most abundant monoisotopic masses of the H3 variants. PTMs as +14 Da (monomethylation), +28 Da (dimethylation) and +42 Da

(trimethylation or acetylation) are the general patterns on the N-terminal residues of histone H3 variants (21). These PTMs were also detected on H3 variants, including H3t, in our data. Several approaches have been undertaken to understand the novel markers and functions associated with histone PTMs during spermatogenesis (22-24). While further research to identify similar modifications (acetylation and trimethylation) and reduce variations between observed and theoretical values is still required, the data presented here provides valuable insight into MS-based characterizations of histone-specific PTMs.

In conclusion, we conducted MS-based top-down analysis to facilitate the comprehensive characterization of histone variants in the mouse testis. Histone variants were successfully separated on a reversed phase column with HFBA. Separated histone variants were characterized by an MS-based top-down approach. In this process, we found four testis-histone variants, H1t, TH2A, TH2B and H3t in the mouse testis when compared to the mouse epididymis and over-expressed H2B and H3 variants were detected in the epididymis. Specifically, approximately 80% of H3.2 was proportionally compensated in the epididymis, as compared to the decreased H3t from the testis. Moreover, our approach showed the masses of PTMs on the histone variant using deconvolution. These results provide information on histone variants in the mouse testis by comprehensive separation and characterization. Our work contributes to the structural and functional research of histone variants in mammalian testes.

Acknowledgements

We thank Thermo-Fisher Scientific K.K. for analytical assistance. A portion of this research was supported by the RIKEN International Program Associate.

References

1. Pradeepa MM, Rao RM. Chromatin remodeling during mammalian spermatogenesis: role of testis specific histone variants and transition proteins. *Soc Reprod Fertil Suppl.* 2007; 63:1-10.
2. Rathke C, Baarends WM, Awe S, Renkawitz-Pohl R. Chromatin dynamics during spermiogenesis. *Biochim Biophys Acta.* 2014; 1839:155-168.
3. Bao J, Bedford MT. Epigenetic regulation of the histone-to-protamine transition during spermatogenesis. *Reproduction.* 2016; 151:R55-R70.
4. Shinagawa T, Huynh LM, Takagi T, Tsukamoto D, Tomaru C, Kwak HG, Dohmae N, Noguchi J, Ishii S. Disruption of Th2a and Th2b genes causes defects in spermatogenesis. *Development.* 2015; 142:1287-1292.
5. Lin Q, Sirotkin A, Skoultchi AI. Normal spermatogenesis in mice lacking the testis-specific linker histone H1t. *Mol Cell Biol.* 2000; 20:2122-2128.
6. Lu S, Xie YM, Li X, Luo J, Shi XQ, Hong X, Pan YH, Ma X. Mass spectrometry analysis of dynamic post-translational modifications of TH2B during

- spermatogenesis. *Mol Hum Reprod.* 2009; 15:373-378.
7. Montellier E, Boussovar F, Rousseaux S, *et al.* Chromatin-to-nucleoprotamine transition is controlled by the histone H2B variant TH2B. *Genes Dev.* 2013; 27:1680-1692.
 8. Zhou H, Ning Z, Starr AE, Abu-Farha M, Figeys D. Advancement in top-down proteomics. *Anal Chem.* 2012; 84:720-734.
 9. Soldi M, Bremang M, Bonaldi T. Biochemical systems approaches for the analysis of histone modification readout. *Biochim Biophys Acta.* 2014; 1839:657-668.
 10. Catherman AD, Skinner OS, Kelleher NL. Top down proteomics: facts and perspectives. *Biochem Biophys Res Commun.* 2014; 445:683-693.
 11. Moradian A, Kalli A, Sweredoski MJ, Hess S. The top-down, middle-down, and bottom-up mass spectrometry approaches for characterization of histone variants and their post-translational modifications. *Proteomics.* 2014; 14:489-497.
 12. Capriotti AL, Cavaliere C, Foglia P, Samperi R, Lagana A. Intact protein separation by chromatographic and/or electrophoretic techniques for top-down proteomics. *J Chromatogr A.* 2011; 1218:8760-8776.
 13. Shibue M, Mant CT, Hodges RS. Effect of anionic ion-pairing reagent hydrophobicity on selectivity of peptide separations by reversed-phase liquid chromatography. *J Chromatogr A.* 2005; 1080:68-75.
 14. Shechter D, Dormann HL, Allis DC, Hake SB. Extraction, purification and analysis of histones. *Nat Protoc.* 2007; 2:1445-1457.
 15. Maehara K, Harada A, Sato Y, Matsumoto M, Nakayama KI, Kimura H, Ohkawa Y. Tissue-specific expression of histone H3 variants diversified after species separation. *Epigenetics Chromatin.* 2015; 8:35.
 16. Feteke S, Veuthey JL, Guillarme D. New trends in reversed-phase liquid chromatographic separations of therapeutic peptides and proteins: theory and applications. *J Pharm Biomed Anal.* 2012; 69:9-27.
 17. Drabent B, Saftig P, Bode C, Doenecke D. Spermatogenesis proceeds normally in mice without linker histone H1t. *Histochem Cell Biol.* 2000; 113:433-442.
 18. Tachiwana H, Osakabe A, Kimura H, Kurumizaka H. Nucleosome formation with the testis-specific histone H3 variant, H3t, by human nucleosome assembly proteins *in vitro*. *Nucleic Acids Res.* 2008; 36:2208-2218.
 19. Sidoli S, Lin S, Karch KR, Garcia BA. Bottom-up and middle-down proteomics have comparable accuracies in defining histone post-translational modification relative abundance and stoichiometry. *Anal Chem.* 2015; 87:3129-3133.
 20. Govin J, Caron C, Lestrat C, Rousseaux S, Khochbin S. The role of histones in chromatin remodelling during mammalian spermiogenesis. *Eur J Biochem.* 2004; 271:3459-3469.
 21. Thomas CE, Kelleher NL, Mizzen CA. Mass spectrometric characterization of human histone H3: a bird's eye view. *J Proteome Res.* 2006; 5:240-247.
 22. Pentakota SK, Sandhya S, Sikarwar AP, Chandra N, Satyanarayana Rao MR. Mapping post-translational modifications of mammalian testicular specific histone variant th2b in tetraploid and haploid germ cells and their implications on the dynamics of nucleosome structure. *J Proteome Res.* 2014; 13:5603-5617.
 23. Brunner AM, Nanni P, Mansuy IM. Epigenetic marking of sperm by post-translational modification of histones and protamines. *Epigenetics Chromatin.* 2014; 7:2.
 24. Mishra LN, Gupta N, Rao SM. Mapping of post-translational modifications of spermatid-specific linker histone H1-like protein, HILS1. *J Proteomics.* 2015; 128:218-230.
- (Received May 19, 2016; Revised August 3, 2016; Accepted August 5, 2016)